Int. J. Solids Structures Vol. 22, No. 10, pp. 1071–1081, 1986
Printed in Great Britain.

0020-7683/86 $3.00+.00
Pergamon Journals Ltd

ELASTIC-PLASTIC SPRINGBACK OF SHEET METALS SUBJECTED TO COMPLEX PLANE STRAIN BENDING HISTORIES

CHIN-CHAN CHU
Ford Motor Company, Dearborn, MI 48121, U.S.A.

(*Received* 17 *December* 1984; *in revised form* 18 *June* 1985)

Abstract—The double-bend technique, which has been experimentally observed to be effective in reducing springback, and which involves a rather complex bending–unbending procedu , is successfully analyzed. This is accomplished by showing that the forming operations produced by most common die configurations can be described by one of three different models constructed herein. These models are analyzed for two classes of material behavior: the standard isotropic hardening type, and one quite general type of anisotropic hardening; this facilitates an assessment of the importance of reversed plastic flow in the springback process. Very good qualitative agreement is observed between the analytical results (for both isotropic and anisotropic hardening) and experimental ones showing the dependence of total springback upon several important parameters. Quantitative discrepancies between the predicted and test results, in the meantime, do decrease as a consequence of the fact that early reversed plastic flow is accounted for in the anisotropic hardening model.

1. INTRODUCTION

The problem that a formed structural sheet tends partially to recover its original state after the forming load is released has long been recognized. Such a deformation occurring upon unloading is generally referred to as "springback". The resultant deviation from a desired shape is most discernible when highly nonuniform deformation, such as bending, is present. Indeed, most of the studies on springback have focused on bending problems. Among these are experimental as well as analytical efforts to define and predict springback under various loading conditions. (See, for example, [1–6].) Most of the existing theoretical work treats only uniform bending problems. The actual situation in practice is, however, much more complicated. In a recent study[7] Wang took into account the nonuniform moment distribution over the full length of a specimen subject to simple flange forming. By doing this, the dependence of springback on parameters such as die gap, which does not appear in a uniform bending model, can be correctly identified.

In this article, a method similar to that in [7] is used to analyze the double-bend technique[8]. Such a technique is selected not only for its effectiveness in reducing springback[9] but also for the relatively complicated loading-reverse loading pattern it introduces. The present complexity is desirable in assessing the appropriateness of the problem-solving methodology proposed here. This analysis also addresses the influence on springback prediction of possible early occurrences of reversed plastic deformation, which was completely neglected in the previously mentioned studies.

Two material hardening models, one isotropic and one anisotropic, are employed. A brief review of these models is given in Section 2. Section 3 describes the problem studied and the mechanisms involved, and also gives a short account of the numerical procedure. The results obtained and some comparisons with experimental data are presented in Section 4.

2. MATERIAL MODELS

The two categories of material models adopted, which differ from one another only when elastic unloading followed by yielding in a different direction occurs, are hereafter referred to as the isotropic and anisotropic models. Note that the word (an)isotropy here only applies to the hardening behavior in different material orientations *during* plastic

deformation. In other words, initial anisotropy, which represents a virgin material's preference of one orientation to another, can be independently accommodated in either model, for example, by the standard anisotropy parameter R for sheet metals. (See, e.g. [13].)

Here a brief discussion of yield surface movement in deviatoric stress space and its application to uniaxial problems is given for each model. A detailed and generalized formulation can be found in [10].

2.1. *Isotropic hardening*

The isotropic hardening model is a widely adopted model which predicts purely elastic springback. According to this model, the yield surface expands isotropically in deviatoric stress space during plastic deformation. This expansion, commonly known as strain-hardening, is reflected by an increase in the subsequent yield stress (flow stress) level. When unloading takes place from a plastic stress state, there can be no further plastic flow until the stress state reaches the expanded yield surface again; that is, until the previously obtained flow stress level is regained.

The application of this model to uniaxial problems is illustrated by dashed curves in Fig. 1. If the uniaxial stress–strain ($\sigma-\varepsilon$) relationship for monotonic loading of a virgin material is written as

$$\sigma = f(\varepsilon),$$

then the unloading behavior, according to the isotropic model, can be described by the following incremental form:

$$\mathrm{d}\sigma = \begin{cases} E\,\mathrm{d}\varepsilon, & \text{for } |\sigma| \leqslant \sigma_f, \\ f'[\varepsilon(|\sigma|)]\,\mathrm{d}\varepsilon, & \text{for } |\sigma| > \sigma_f. \end{cases}$$

Here $\mathrm{d}\sigma$ and $\mathrm{d}\varepsilon$ denote increments of σ and ε, respectively, f' denotes the differentiation of f with respect to its argument, $|\sigma|$ denotes the absolute value of σ, E is Young's modulus, and σ_f is the previously obtained flow stress level.

Although it is well recognized that the isotropic hardening model is insufficient for modelling the Bauschinger effect, it is simple to employ and serves as a good approximation when reversed loading occurs only to a limited extent.

2.2. *Anisotropic hardening*

An anisotropic model which is compatible with all basic features of metal plasticity and which can describe Bauschinger's effect is also adopted here. This model assumes a

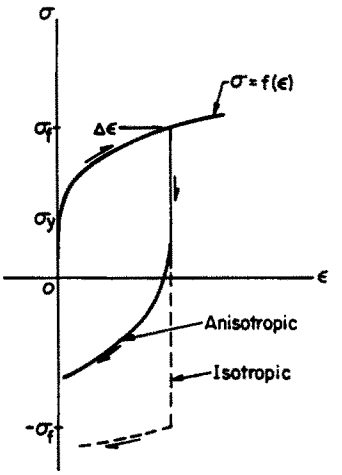

Fig. 1. A typical uniaxial stress–strain relationship for loading and unloading, as predicted by both the isotropic and anisotropic hardening models.

continuous distribution of yield surfaces in deviatoric stress space. The size of the *active* yield surface, on which the current stress state lies, determines the flow stress level. At the material's virgin state, the surfaces are concentric about the zero stress state. During plastic deformation, the stress state advances to progressively larger yield surfaces, and the largest yield surface in contact with the current stress state becomes the active one. In the meantime, the evolving stress state pushes all the smaller yield surfaces forward so that they become tangent to the active yield surface at the loading point. The material thus keeps a memory of the loading history via the distribution of yield surfaces in deviatoric stress space after plastic deformation. When unloading occurs, it is the smallest yield surface, whose size is related to the initial yield stress, that the stress state will first encounter to initiate reversed plastic flow.

While experimental data are difficult to obtain to support such an anisotropic progression of the active yield surface during a complicated plastic loading history, many macroscopically observed cyclic phenomena, mainly from uniaxial testing, can be well modelled by the aforementioned yield surface field concept. The concept was originally proposed by Mróz[11] and recently generalized to three-dimensional problems in [10].

Here again only the uniaxial case is used as an illustration. The solid curve in Fig. 1 shows an early plastic response upon unloading as derived from the anisotropic model. In an incremental form, we have

$$d\sigma = \begin{cases} f'(\tfrac{1}{2}|\Delta\varepsilon|)\,d\varepsilon, & \text{for } |\sigma| \leqslant \sigma_f, \\ f'[\varepsilon(|\sigma|)]\,d\varepsilon, & \text{for } |\sigma| > \sigma_f. \end{cases}$$

The first part of this equation coincides with the experimental observation that the unloading stress–strain curve is approximately the twofold magnification of the monotonic curve.

Note that the current anisotropic model is not the only one of its kind. In fact, the two-surface theory has been more widely discussed (see, for example, [12]). However, it can be readily shown that the two-surface theory is a special case of the generalized formulation in [10].

A problem which will be discussed in detail later involves the bending of a *wide thin* sheet. Four basic assumptions used here are

(1) Plane-strain conditions are approached in the width direction.
(2) Plane-stress conditions prevail in the thickness direction.
(3) Normal sections remain normal during bending.
(4) The shift of the neutral surface during bending and unbending is negligible. (This was found to be a very good approximation for thin sheets even under severe bending[7].)

The plane-stress and plane-strain conditions simplify the problem to essentially a uniaxial one. That is, if Hill's anisotropic yield criterion (Hill[14]) is adopted for sheet metal with initial anisotropy parameter R, the fiber stress σ_F is related to the effective stress σ only by a proportionality constant:

$$\sigma = \sqrt{(1+2R)/(1+R)}\,\sigma_F.$$

A moment–curvature $(M-k)$ curve having a shape similar to that of the stress–strain curve in Fig. 1 is thus immediately obtainable by utilizing the stress–strain relationship presented above. Such curves are plotted in Fig. 2 for three types of steels: HS110, *D*ual *P*hase and *A*l-*K*illed *D*raw *Q*uality steels. (The material constants used are taken from [7].) The unbending portion of the curve is displayed in the figure for HS110 and DP steels. The solid and dashed curves are for the anisotropic and isotropic models, respectively. It is observed that the difference between the two models increases for materials with higher strain-hardening exponents and/or lower yield stresses. The difference, however, starts to decrease as unloading continues into the range where both models predict plastic behavior. With such a moment–curvature relationship established, the amount of computation necess-

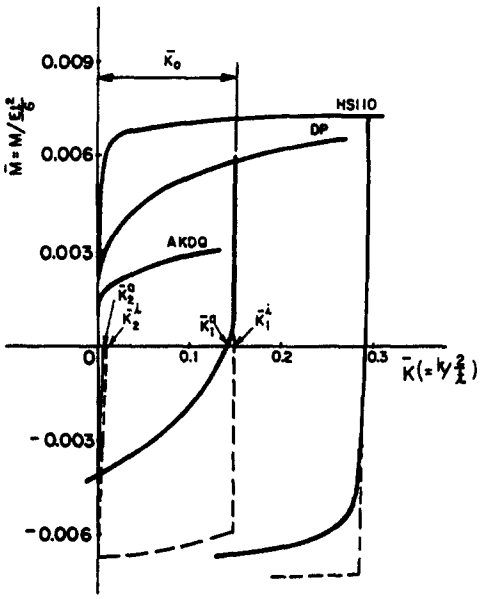

Fig. 2. The normalized moment–curvature curves for HS110, DP and AKDQ steels. The solid and dashed curves are for the anisotropic and the isotropic model, respectively.

ary for springback prediction can be significantly reduced. As will be exemplified later, for special cases, such as problems with zero die-clearance, analytical solutions can even be acquired without resorting to numerical computations.

3. PROBLEM FORMULATION

The problem to be analyzed here is the double-bend technique, recently proposed by Liu[8] to reduce springback resulting from simple flange forming. The loading-reverse loading combination involved in this technique provides an ideal case study for the applicability of the proposed modelling methodology as well as for the accumulated effects on springback prediction from elastic-plastic unloading.

As sketched in Fig. 3, a planar sheet which is wide in the z-direction is first bent at A to a constrained shape [the solid curve in Fig. 3(a)] and allowed to spring back [to the dashed position in Fig. 3(a)] when the bending force is released. The sheet is then moved out of the die horizontally by a distance h and bent at B to a second constrained position, the solid curve in Fig. 3(b). The final shape to which the sheet recovers after the release of

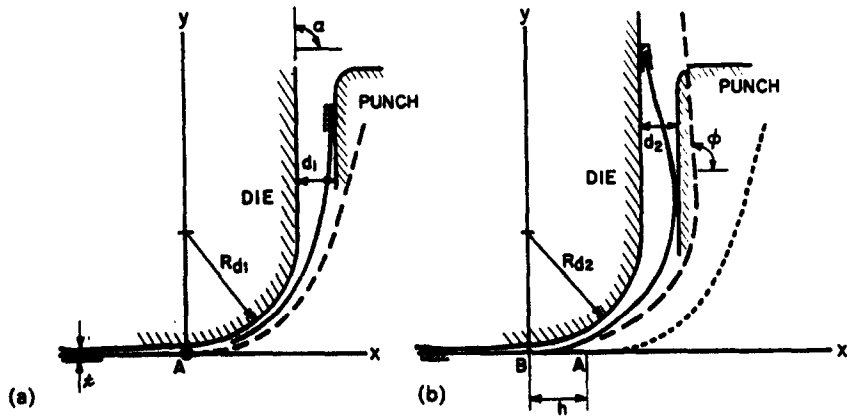

Fig. 3. Schematic diagram of: (a) the first operation, and (b) the second operation of the double-bend technique.

the second bending force [the dashed curve in Fig. 3(b)] makes an angle $\Phi(y)$ with the x-axis. The total springback angle θ is then measured by the difference between Φ of the upper flange wall and the die angle α; that is, $\theta = \alpha - \Phi(y_u)$. The die angle α is arbitrarily chosen as 90° in the current study.

The objective is to analyze the operation and to determine the dependence of the final shape on problem parameters, such as the distance h between bending sites A and B, the die gap d, the die radius r_d, and the sheet thickness t. The first operation is a simple flange forming process which was analyzed in [7] via an isotropic hardening model. Here the analysis is repeated by employing the anisotropic model discussed in Section 2 to show the influence of hardening models on simple springback and to prepare for the analysis of the second operation.

The initial state of the second strike consists of a partly deformed and partly virginal sheet. Depending on the degree of contact the sheet makes with the punch and die, one of the three mechanisms discussed below applies. The flange wall position and the moment distribution associated with each of the mechanisms are schematically represented in Fig. 4.

In the most simple mechanism, as shown in Fig. 4(a), there is no contact between the sheet and the die beyond point S and only one point of contact at C between the sheet and the punch. Therefore, similar to the situation in simple flange forming, we have the separation point S which marks the upper bound of an area bent to constant curvature and the end point C where a bending force is exerted on the sheet via the punch. The boundary conditions for this mechanism are

$$k(y) = (r_{d2} + t/2)^{-1} = k_0, \qquad \text{for} \quad 0 \leqslant y \leqslant y_s, \tag{1a}$$

$$x(y_c) = r_{d2} + d_2 - t/2 = x_c \tag{1b}$$

and

$$\Phi(y_c) = \pi/2 = \Phi_c. \tag{1c}$$

Note that eqns (1) are written for the neutral axis of the sheet. Solutions through the thickness can be obtained by using Assumptions (3) and (4) mentioned in the previous section.

The moment resulting from the bending force at C is a linear function of y between y_s and y_c:

$$M(y) = M_c + (M_s - M_c)(y_c - y)/(y_c - y_s), \qquad \text{for} \quad y_s \leqslant y \leqslant y_c. \tag{2}$$

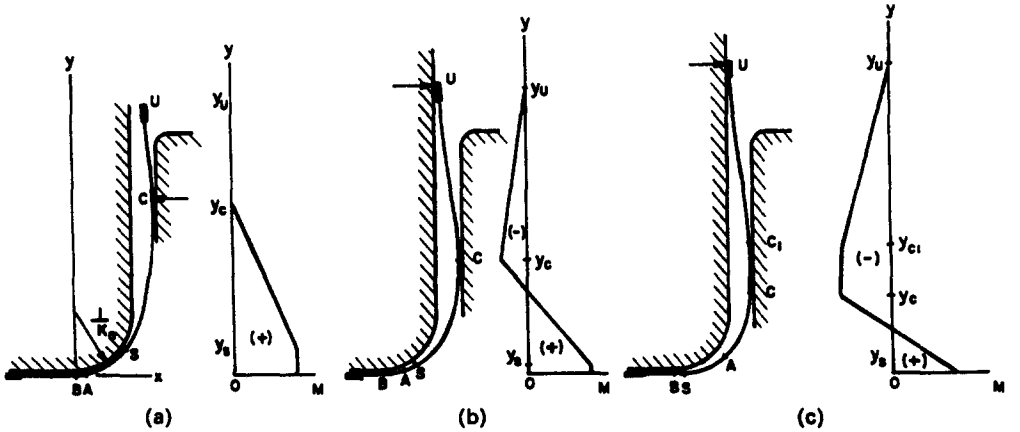

Fig. 4. Schematic diagram of the second operation and its associated moment distribution for: (a) the first, (b) the second, and (c) the third mechanism.

Here $M_c = 0$ and $M_s = M_0$, with M_0 being the constant moment required to bend the sheet to constant curvature k_0 for $0 \leqslant y \leqslant y_s$.

A numerical solution can be obtained by dividing the sheet along its neutral axis into segments and using a trial-and-error method. First, a combination of y_s and y_c is assumed. These values are subsequently revised until the resultant x_c and Φ_c satisfy eqns (1b) and (1c), respectively.

For special cases with $y_s = 0$, M_s in eqn (2) is determined only to be no greater than M_0. It is then the correct M_s and y_c, instead of y_s and y_c, which are sought.

The second mechanism is similar to the first, but with the additional slight complication produced by the unbending force from the die wall at U, as displayed in Fig. 4(b). In addition to eqns (1) and (2), we have

$$x(y_u) = r_{d2} + t/2 \tag{3}$$

and

$$M(y) = M_c(y_u - y)/(y_u - y_c). \tag{4}$$

We now search for a combination of y_s, y_c and M_c which satisfies eqns (1b), (1c) and (3). Note that in the current formulation the length of the sheet is not a problem variable. Instead, it is taken to be large enough so that eqn (1c) is satisfied in the first operation. This length determines the relative position of U with respect to C in the second operation. The die force at U and thus the linear moment distribution between C and U in the second (and third) mechanism are determined to be just large enough to unbend this upper portion of the sheet from its finite initial curvature to a shape compatible with the die gap.

The third mechanism is similar to the second except that the contact between the sheet and the punch occurs along a section instead of just at a point. That is, the sheet between C and C_1 is unbent to conform with the punch wall curvature (which is zero here), as shown in Fig. 4(c). With the curvature specified, the moment $M(y)$ for $y_c \leqslant y \leqslant y_{c1}$ can be obtained from the $M-k$ curve. By replacing the subscript C in eqn (4) by C_1, the solution method for the second mechanism is then applicable to the third case.

After the moment distribution is completely determined for both the first and the second operations, the total springback can be calculated from the M–k curve by integrating along the sheet axis the curvature change caused by release of the bending or unbending moment.

4. RESULTS

In this section results illustrating effects of several problem parameters and material models on total springback angle are summarized.

First, the difference between the two material models are well exemplified in Fig. 5 where the springback angle measured after simple flanging is plotted against the die gap–thickness ratio for two materials. (In this and later figures, the solid and dashed curves display results from the anisotropic and isotropic models, respectively.) For HS110 steels, which have high yield stresses and low strain-hardening exponents, there is no difference between the two models in predicting simple flanging springback. The resulting elastic springback is seen to agree extremely well with experimental data, which are indicated by open triangles. For materials with high strain-hardening exponents, such as DP steels, results from the two models can differ significantly as a consequence of plastic behavior accounted for by the anisotropic hardening rule but not by the isotropic hardening rule. The better correlation between the anisotropic model and experimental results (presented by open circles) for DP steels in Fig. 5 indicates the important role played by plastic behavior during reverse loading for high strain-hardening materials. It should be pointed out that the difference between the anisotropic and isotropic models also depends on the loading history. As will be shown in the following examples of the double-bend technique,

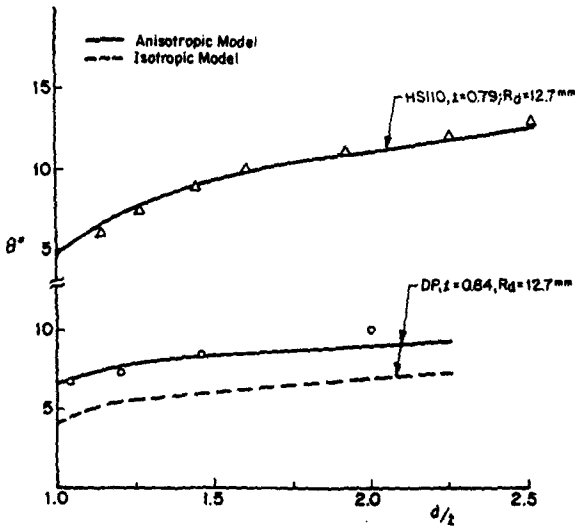

Fig. 5. Analytical and experimental results of springback for simple flange forming as a function of die gap–thickness ratio for HS110 and DP steels.

the difference between the two models is cumulative and hence can increase by a significant amount when the bending mechanism becomes more complicated.

The dependence of the total springback angle of the double-bend technique, θ, on the distance h between the first and second bending sites is displayed in Fig. 6. For all materials, the springback angle is predicted to drop rapidly from its value for simple flange forming when h increases from zero. Here the first of the three previously mentioned mechanisms applies. The rate of the springback angle reduction for small h can be obtained analytically, as shown in the Appendix, to be k_1, the residual curvature in a material element after it is subjected to bending moment M_0.

As h continues to increase, the curve reaches a rather flat region before a final small,

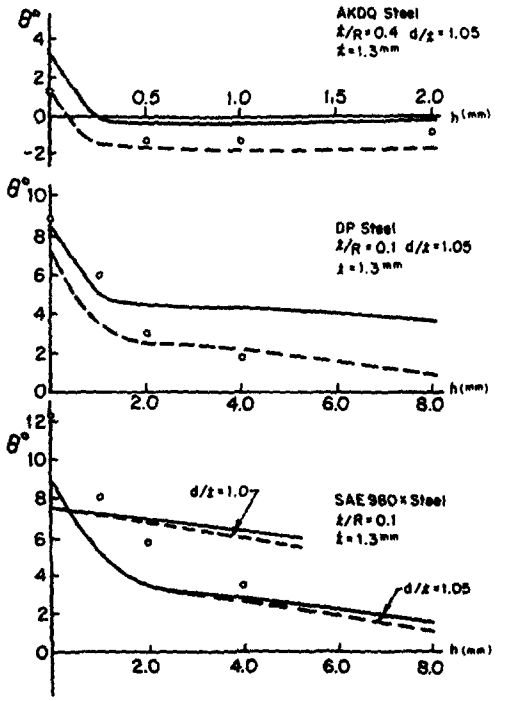

Fig. 6. Analytical and experimental[6] results of total springback angle for the double-bend technique as a function of the shift of bending sites for: (a) AKDQ, (b) DP, and (c) SAE 980X steels.

constant negative slope is attained. Here the second and the third mechanism applies, respectively. The final slope, as analyzed in the Appendix, is k_2, the residual curvature in a material element subjected to bending moment M_0 followed by complete unbending (to zero curvature).

The analysis used in the Appendix can also be applied to problems with zero die-clearance ($d = t$). For this special case, it is easy to show that θ depends linearly on h. One such example is displayed in Fig. 6(c) for SAE 980X steels. The constant slope is k_2. The seemingly sharp difference between the curves for $d/t = 1.0$ and $d/t = 1.05$ in Fig. 6(c) is in fact a result of diminishing control of the first and second mechanisms, which, as discussed above, occur in the small-h range, in reducing springback when d/t approaches unity. The importance of die gap in springback modelling is thus clearly demonstrated in the figure. This aspect will be examined more closely later.

The above-mentioned dependence of θ on h is predicted by both models. As expected, the anisotropic results are consistently higher than the isotropic results. The difference between the two models is seen to increase as the loading history becomes more complicated; that is, as h increases in Fig. 6. Comparing with the few experimental data available[6], represented by open circles in the figure, only qualitative agreement is observed. The lack of a quantitative match, meaning that no conclusion on appropriateness of material models can be made, is attributed to two facts: First, no stress–strain relationship was reported in [6]; second, the control of the problem geometry exercised in [6] is at times not identical with that assumed in the present analysis. For instance, in [6], the sheet was not always locked to the die up to the bending site B. Recoiling, which allows the curvature of elements near B to be much smaller than that in eqn (1a), might have taken place and hence significantly changed the moment distribution through the sheet length.

According to Fig. 6, depending on the material and problem parameters, springback may not be completely eliminated by a large bending site shift. In showing the effect of die gap on total springback (with h fixed at the large value of 2.0 mm) in Fig. 7, it is revealed that further springback reduction can be achieved by adjusting die gap d_2. The θ–d_2 curve has a V-shape. For large d_2, the first mechanism applies and the curve approaches the limit simple flange forming value, denoted in the figure by subscript 1. As d_2 decreases, the second and then the third mechanism takes over. The increase in complexity of the mechanisms, as discussed earlier, results in the difference between predicted springback angles from the

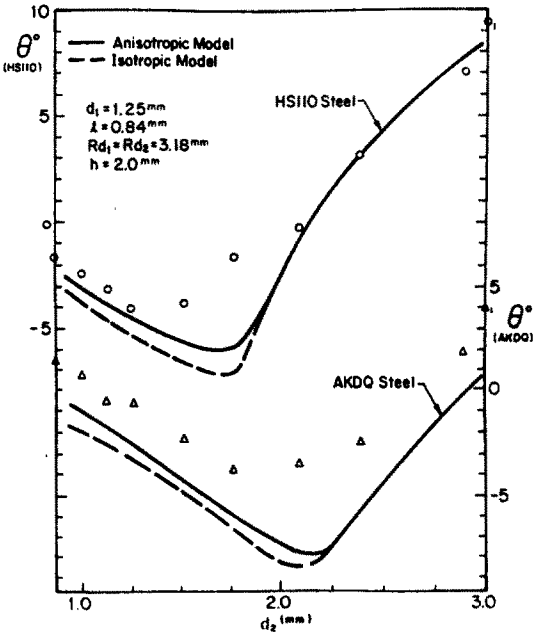

Fig. 7. Analytical and experimental[9] results of total springback angle for the double-bend technique as a function of the die gap in the second operation for HS110 and AKDQ steels.

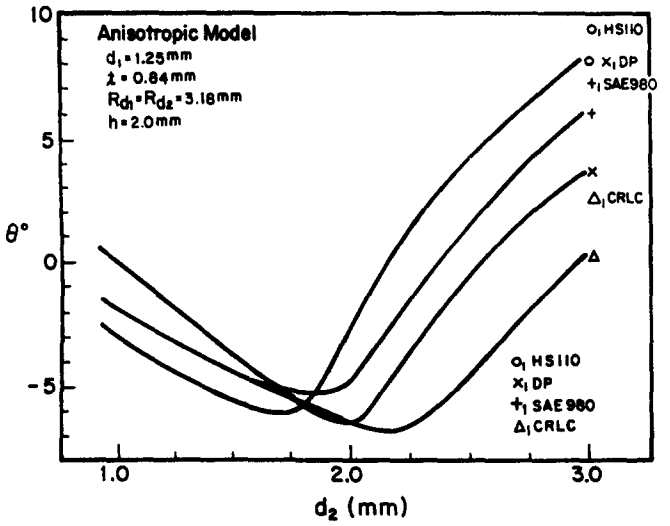

Fig. 8. Predicted springback angle for the double-bend technique as a function of the die gap in the second operation, via the anisotropic hardening model, for several sheets.

two models for small d_2. The shape of the θ–d_2 curve is in good agreement with experimental results, with the largest discrepancy occurring near the minimum-θ region where the second-mechanism governs. Again, at least part of the quantitative difference between the theory and experiments can be attributed to lack of information on the stress–strain relationships for materials actually tested.

The same θ–d_2 curves based on the anisotropic model are plotted for four different materials in Fig. 8. Observe that the minimum springback angle attained seems to be much less sensitive to the material than is simple flange springback. In Fig. 9, θ–d_2 curves obtained from both models for DP steels show the large influence derived from the t–R_d ratio.

Finally, to give an example of the applicability of the current methodology to other similar bending problems, the effect of changing die radius in the second operation (to a smaller one) on total springback is explored. This technique, generally referred to as spanking, is shown in Fig. 10 for DP steels to be very powerful in reducing springback. Three d/t-values are used to demonstrate once again the important role played by die gap in a practical situation.

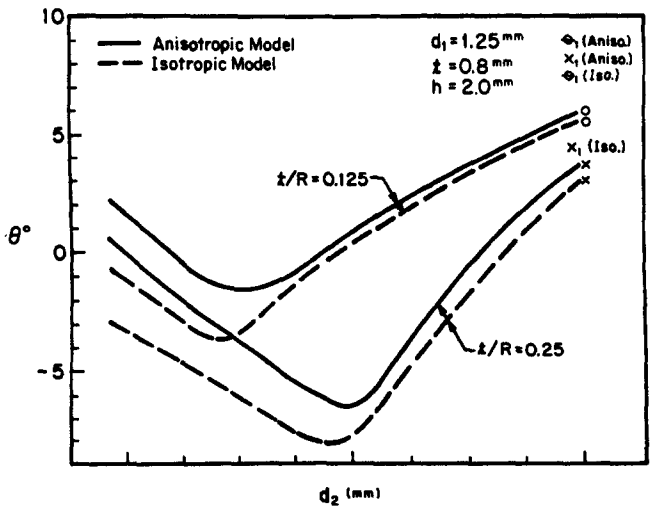

Fig. 9. Predicted springback angle for the double-bend technique as a function of the die gap in the second operation, via the anisotropic model, for two thickness–die radius ratios.

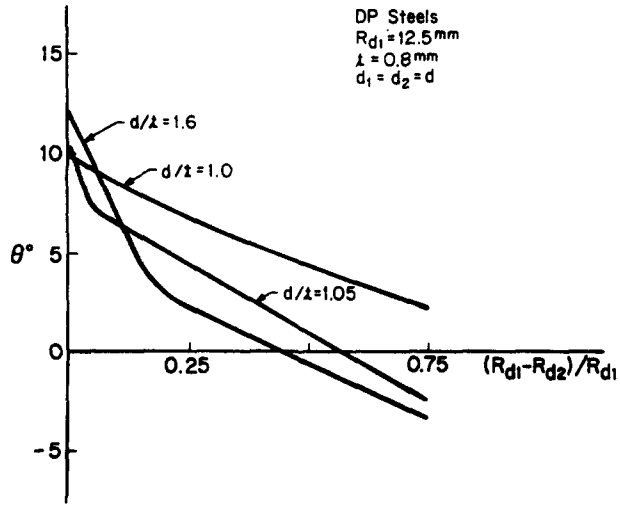

Fig. 10. Predicted springback angle for the spanking technique as a function of the variation in die radius, via the anisotropic model, for three die gap–thickness ratios.

5. DISCUSSION

The main results of this study are

(1) The problem solving technique introduced, which involves the construction of various working mechanisms for different situations, is shown to be accurate in modelling springback phenomena after simple flange forming. Further applications to more complex problems such as curling and bead force calculation are desirable.

(2) Early plastic deformation upon unloading can be better described by an anisotropic hardening model than by the standard isotropic hardening one. The anisotropic model is shown to be easy to employ. The difference between the two models is found to be quantitative but not qualitative. The quantitative improvement in springback prediction appears to be significant only for materials with high strain-hardening exponent and/or for materials subjected to complicated loading-reverse loading histories.

Finally, it should be pointed out that one factor which was not included in the present analysis is the specimen length. While the influence of specimen length on springback modelling can be easily assessed for a simple flanging operation, its role in the double-bend technique with large bending site movement is more involved, as observed in experiments currently being conducted. There, as well as in more complicated problems yet to be treated, a fourth and probably more mechanisms are required for a complete analysis.

REFERENCES

1. F. J. Gardiner, The spring back of metals. *Trans. ASME* **79**, 1 (1957).
2. W. Schroeder, Mechanics of sheet-metal bending. *Trans. ASME* **79**, 817 (1957).
3. J. L. Duncan and J. E. Bird, Approximate calculations for draw die forming and their application to aluminum alloy sheet. Proc. 10th Biennial Congress IDDRG, Warwick, England, p. 45 (1978).
4. W. Johnson and A. N. Singh, Springback in circular blanks. *Metallurgia* **47**, 275 (1980)
5. M. L. Wenner, On work hardening and springback in plane strain draw forming. *J. Appl. Metalworking* **2**, 277 (1983).
6. R. G. Davies and Y. C. Liu, Control of springback in a flanging operation. *J. Appl. Metalworking* **3**, 142 (1984).
7. N. M. Wang, Efficiency in sheet metal forming. Proc. 13th Biennial Congress IDDRG, Melbourne, Australia, p. 133 (1984).
8. Y. C. Liu, U.S. Patent No. 4373371, Feb. 1983.
9. Y. C. Liu, Springback reduction in U-channels—double-bend technique. *J. Appl. Metalworking* **3**, 148 (1984).
10. C. C. Chu, A three-dimensional model of anisotropic hardening in metals and its application to the analysis of sheet metal formability. *J. Mech. Phys. Solids* **32**, 197 (1984).
11. Z. Mróz, On the description of anisotropic workhardening. *J. Mech. Phys. Solids* **15**, 163 (1967).
12. R. D. Krieg, A practical two surface plasticity theory. *J. Appl. Mech., Trans. ASME* **42**, 641 (1975).
13. P. B. Mellor, Sheet-metal forming. *Int. Metals Rev.* **26**, 1 (1981).
14. R. Hill, *The Mathematical Theory of Plasticity*. Oxford University Press, London (1950).

APPENDIX

In the second operation of the double-bend technique, by keeping the die setup unchanged and by varying the bending site movement, the dependence of total springback on h can be obtained. For very small h, the first mechanism sketched in Fig. 4(a) applied. Due to the bending of the new material between A and B, the position of point C, where Φ is equal to 90°, must be lower for the second bending than that in the first operation. That is, the material between A and C is subject to a moment less than or equal to its previous value in the first bending. According to both models, the material within this region completes a small moment–curvature cycle and returns to its initial state. The net effect of the second operation on total springback therefore derives from bending of the virgin material between A and B, which is within the constant moment region. If we denote the residual curvature in such a material element by k_1, of which the normalized value $\bar{k}_1$ is illustrated in Fig. 2 for DP steels, the total springback reduction for small h is

$$\Delta\theta = \bar{k}_1(2/t)\,\Delta h = k_1\,\Delta h,$$

where Δ denotes the variation of a quantity.

As h becomes very large the third mechanism sketched in Fig. 4(c) controls. In this case, the numerical solutions show that as h varies, the y-coordinates of S and C do not change. Therefore, the bending and unbending of the lower portion of the sheet makes no contribution to further springback reduction. The difference in the unbending moment for the upper portion of the sheet from C to U caused by the h-increment occurs only in a region of length Δh immediately above C. Since we also learn from the numerical solutions that C is within the constant moment region during the first operation, the effect of its complete unbending on the springback angle is obtained as $(k_2\,\Delta h)$, with k_2 defined as the residual curvature in a material element subject to bending moment M_0 followed by complete unbending. The normalized value $\bar{k}_2$ is illustrated in Fig. 2 for DP steels.